AMERICAN SOCIETY FOR MICROBIOLOGY | Applied and Environmental Microbiology®

ENVIRONMENTAL MICROBIOLOGY

# Transformative Approach To Investigate the Microphysical Factors Influencing Airborne Transmission of Pathogens

Mara Otero Fernandez,[a] Richard J. Thomas,[b] Henry Oswin,[a] Allen E. Haddrell,[a] Jonathan P. Reid[a]

[a]School of Chemistry, University of Bristol, Bristol, United Kingdom
[b]Defence Science Technology Laboratory (DSTL), Porton Down, Salisbury, United Kingdom

**ABSTRACT** Emerging outbreaks of airborne pathogenic infections worldwide, such as the current severe acute respiratory syndrome coronavirus 2 (SARS-CoV-2) pandemic, have raised the need to understand parameters affecting the airborne survival of microbes in order to develop measures for effective infection control. We report a novel experimental strategy, TAMBAS (tandem approach for microphysical and biological assessment of airborne microorganism survival), to explore the synergistic interactions between the physicochemical and biological processes that impact airborne microbe survival in aerosol droplets. This innovative approach provides a unique and detailed understanding of the processes taking place from aerosol droplet generation through to equilibration and viability decay in the local environment, elucidating decay mechanisms not previously described. The impact of evaporation kinetics, solute hygroscopicity and concentration, particle morphology, and equilibrium particle size on airborne survival are reported, using *Escherichia coli* MRE162 as a benchmark system. For this system, we report that (i) particle crystallization does not directly impact microbe longevity, (ii) bacteria act as crystallization nuclei during droplet drying and equilibration, and (iii) the kinetics of size and compositional change appear to have a larger effect on microbe longevity than the equilibrium solute concentration.

**IMPORTANCE** A transformative approach to identify the physicochemical processes that impact the biological decay rates of bacteria in aerosol droplets is described. It is shown that the evaporation process and changes in the phase and morphology of the aerosol particle during evaporation impact microorganism viability. The equilibrium droplet size was found to affect airborne bacterial viability. Furthermore, the presence of *Escherichia coli* MRE162 in a droplet does not affect aerosol growth/evaporation but influences the dynamic behavior of the aerosol by processing the culture medium prior to aerosolization, affecting the hygroscopicity of the culture medium; this highlights the importance of the inorganic and organic chemical composition within the aerosolized droplets that impact hygroscopicity. Bacteria also act as crystallization nuclei. The novel approach and data have implications for increased mechanistic understanding of aerosol survival and infectivity in bioaerosol studies spanning the medical, veterinary, farming, and agricultural fields, including the role of microorganisms in atmospheric processing and cloud formation.

**KEYWORDS** atmospheric bioaerosols, bacterial viability, electrodynamic balance

The airborne route of transmission of respiratory infectious diseases has been identified as the major transmission mode in many epidemics, predominantly in indoor environments (1–6). Nevertheless, the mechanisms that control the survival of airborne respiratory pathogens remain largely unknown due to the complex multifactorial processes involved (7). Further investigation to determine the fundamental mechanisms of airborne disease transmission is critical, not only for developing strat-

**Citation** Otero Fernandez M, Thomas RJ, Oswin H, Haddrell AE, Reid JP. 2020. Transformative approach to investigate the microphysical factors influencing airborne transmission of pathogens. Appl Environ Microbiol 86:e01543-20. https://doi.org/10.1128/AEM.01543-20.

**Editor** Christopher A. Elkins, Centers for Disease Control and Prevention



Address correspondence to Allen E. Haddrell, a.haddrell@bristol.ac.uk., or Jonathan P. Reid, j.p.reid@bristol.ac.uk.

**Received** 7 July 2020
**Accepted** 17 September 2020
**Accepted manuscript posted online** 25 September 2020
**Published** 10 November 2020

egies to mitigate the impact of disease outbreaks but also for understanding the seasonality of infectious diseases (8), improving the treatment of respiratory infections (9), and even determining the synergistic effects of air pollution on the atmospheric microbial community (10).

Some of the critical factors that are thought to affect microbial survival in the aerosol phase include relative humidity (RH), temperature, particle size, and microbial load (11–19). Further, experimental methods of aerosol generation (i.e., reflux nebulizers) and sampling (i.e., impingement) can introduce damage to microorganisms. Thus, the aerosolized population may not be wholly representative of microorganisms aerosolized naturally through a cough or sneeze (20–24). However, the CELEBS (controlled electrodynamic levitation and extraction of bioaerosol onto a substrate) system minimizes the damage imparted during aerosol generation and sampling, meaning that biological decay is due purely to the environment and droplet conditions (25).

To address the fundamental mechanistic questions central to the understanding of airborne disease transmission, we present a new approach derived from the use of two complementary experimental tools. First, the aerosol droplet evaporation kinetics, changes in particle morphology during drying, and changes in solute hygroscopicity are fully quantified using the comparative kinetic electrodynamic balance (CK-EDB), providing detailed understanding of the dynamic behavior of aerosol particles (26, 27). Second, the bioaerosol survival rates of identical particle types as a function of time, particle composition, and environmental conditions are measured with the CELEBS system (25). When used in combination, these particle levitation technologies can be used to interrogate the true airborne state of airborne microorganisms. Understanding this state is critical, since the physicochemical conditions to which microorganisms are exposed within an aerosol host droplet can differ dramatically from those in a bulk phase sample (28), potentially impacting their viability and, consequently, their transmissibility between hosts. Combining the strengths of these complementary methodologies for probing aerosol particles directly, the tandem approach for microphysical and biological assessment of airborne microorganism survival (TAMBAS) enables an exploration of the complex interconnections between airborne microphysics and biological decay.

## RESULTS

The capability of our novel approach, described in Materials and Methods and the supplemental material, is assessed through combined measurements of the dynamics driving the evolving size, composition, morphology, and hygroscopic response, with their corresponding biological outcomes. We illustrate the value of this approach by reporting the outcomes of studies to explore the coupling of aerosol microphysical and biological processes using *Escherichia coli* MRE162 as a benchmark system, representing the survival rates as a decline in culturability as described in Materials and Methods.

**Water content of microbiological media: bacterial processing of growth media affects aerosol hygroscopicity.** Retrieval of the equilibrium hygroscopic properties of microbial media from mass transfer kinetics measurements was performed by the CK-EDB method (26, 29). The relationship between water activity and aerosol composition for common microbial media is compared to thermodynamic model predictions for NaCl (extended aerosol inorganics model [E-AIM] [30]) (Fig. 1). Freshly autoclaved LB broth and LB broth previously used to culture bacteria over 24 h with subsequent withdrawal of *E. coli* MRE-162 cells are referred to as nonmetabolized and metabolized, respectively. The hygroscopic growth curves in Fig. 1 show that phosphate-buffered saline (PBS) has similar hygroscopicity to NaCl alone (NaCl makes up 83% of the mass of PBS). However, both LB broth solutions, with 60% of the solute mass arising from organic components, are much less hygroscopic. Interestingly, nonmetabolized and metabolized LB broth solutions display different hygroscopicities, suggesting that the metabolization of LB broth by bacteria alters the solute composition and, thus, the water content of aerosol droplets at a particular RH. Although it is well known that

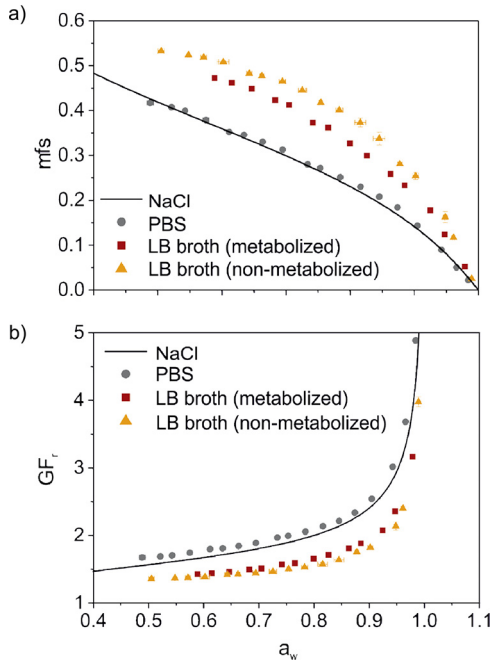


**FIG 1** Hygroscopicity curves of different culture media with variation in solution water activity ($a_w$), presented in terms of the mass fraction of solute (mfs) (a) and the radial growth factor ($GF_r$) (b). Predicted curves for NaCl hygroscopicity (lines) from E-AIM are also shown for reference.

bacteria alter the composition of media through metabolism, the effect that this has on aerosol hygroscopicity is a novel observation. Ostensibly, microbes affect the physicochemical properties of bioaerosols, altering the initial solute composition.

In these studies, the microbial media used to generate aerosol droplets in order to investigate compositional changes as a function of the ambient RH are not representative of respiratory droplets responsible for, for example, human-to-human transmission mechanisms. However, this investigation allows us to correlate droplet compositions with different characteristics (e.g., a nutrient-rich medium, such as LB broth, compared to a nutrient-poor medium, such as PBS) and determine whether the components play a role in the airborne survival of microorganisms. In addition, aerobiological studies have been performed since the late 1950s (31) by using different microorganisms in a wide variety of suspending fluids, from water (32), growth medium (17, 33), and PBS (34) to more-representative biological compositions, such as artificial saliva (35, 36). However, most studies do not directly compare these solutions within a single study, and therefore, the effect of composition is still largely unknown.

**Changes in phase/morphology and solute concentration during droplet evaporation at varying RHs affect microorganism viability.** The evaporation profiles (including changes in morphology) of nonmetabolized individual LB broth droplets (Fig. 2a) and PBS droplets (Fig. 2b) at RHs of 30%, 50%, and 70% were investigated. For evaporating LB broth solution droplets, light-scattering analysis (37) suggests the formation of NaCl inclusions (NaCl makes up 40% of the mass of LB broth) during evaporation at RHs of 30 and 50%, while complete homogeneity is sustained during evaporation at 70% RH (Fig. 2a). PBS solution droplets remain homogeneous during evaporation at RHs of 50% and above, but crystal formation is observed for evaporation at an RH of 30% (Fig. 2b, red point); at this RH, it is not possible to determine the size of the crystallized nonspherical particle (27). As expected, efflorescence of PBS took place between 30 and 50% RH, which agrees with the known efflorescence RH for NaCl (45 to 50%) (38). In both Fig. 2a and b, the morphology analysis is most certain after the droplets reach equilibrium with their environment, i.e.,

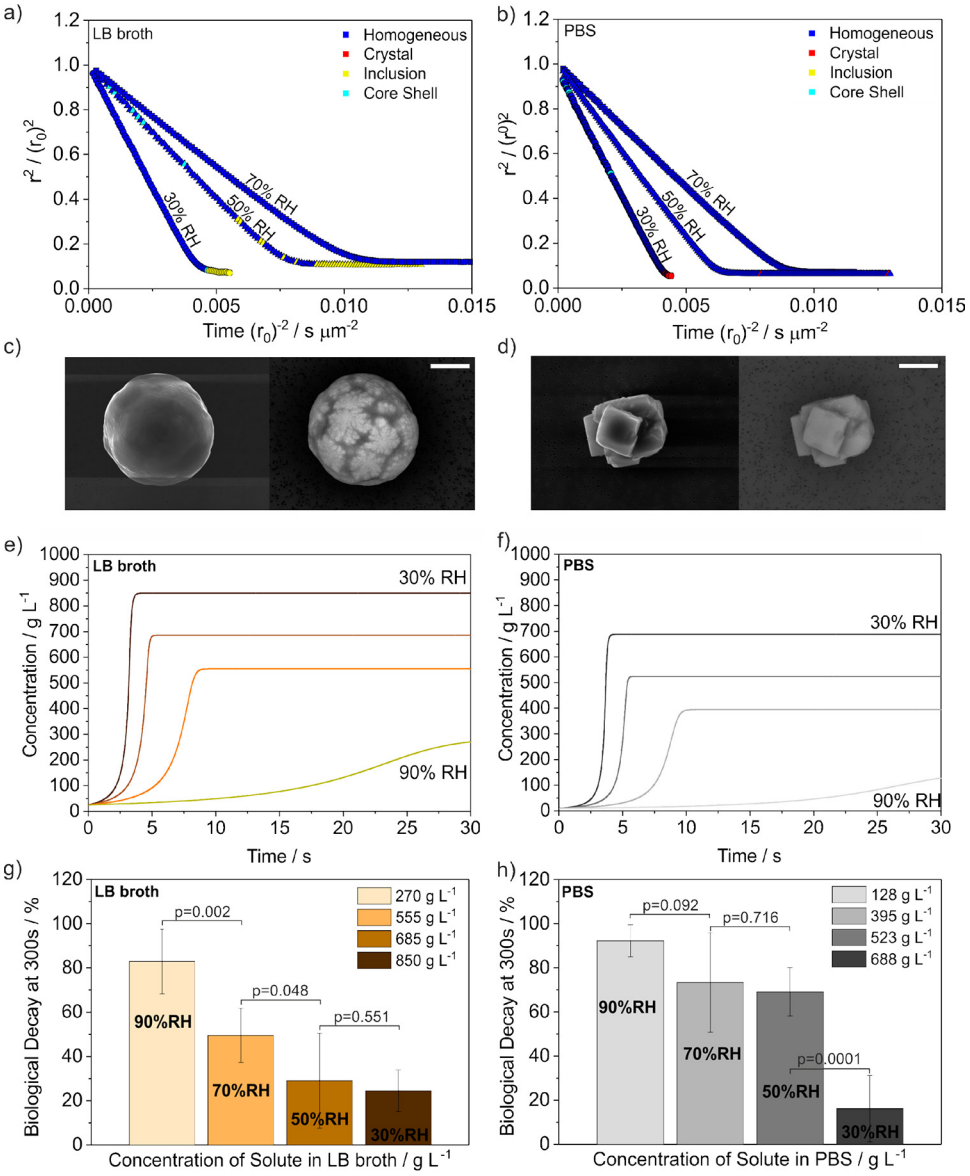


**FIG 2** (a and b) Evolution of size and morphology for droplets of nonmetabolized LB broth (a) and PBS (b) evaporating at 30%, 50%, and 70% gas-phase RHs. Slopes for the linear trend in the radius-squared are −216.7, −118.1, and −90.4 in the case of LB broth droplets and −221.9, −153.4, and −108.7 for PBS droplet composition, each at 30, 50, and 70% RHs, respectively. (c and d) SEM and backscattered electron images for particles formed from nonmetabolized LB broth (c) and PBS (d) at 30% RH. (e and f) Predicted time-dependent solute concentrations for evaporation of droplets of nonmetabolized LB broth (e) and PBS (f) into gas phases with RHs spanning 30% to 90% at 20°C. To simulate the evaporation profiles, a starting radius of 25 $\mu$m and concentrations of 25 g liter$^{-1}$ and 9.5 g liter$^{-1}$ for LB broth and PBS, respectively, were used. (g and h) The impact of morphology and solute concentration on the viability of airborne bacteria at 300 s from droplet generation and at RHs of 30% to 90% are shown for LB broth (g) and PBS (h) droplets containing *E. coli* MRE162 [starting concentration, (2.6 ± 0.6) × 10$^8$ CFU ml$^{-1}$, or 28 ± 11 CFU droplet$^{-1}$]. The *P* values obtained by comparing the compositions of LB broth and PBS at 90, 70, 50, and 30% RHs by applying a two-sample *t* test are 0.137, 0.079, 0.00, and 0.22, respectively, showing a significant difference in survivability between compositions only at 50% RH.

once the cumulative phase functions become consistent, making the phase identification more robust.

To further explore the morphologies formed from the drying of PBS and LB broth droplets at 30% RH, particles were captured for scanning electron microscopy (SEM) analysis (Fig. 2c and d). The morphologies are as expected from the light-scattering analysis performed with the CK-EDB measurements. Briefly, LB broth particles are broadly spherical (Fig. 2c; see also Fig. S4a in the supplemental material) with clear

evidence of dendritic salt inclusions, reflecting the likely diffusional limitation due to elevated particle viscosity of these organic-material-rich droplets formed upon rapid drying as inclusions form (mass fraction of solute of organic compounds, 60%) (39, 40). In contrast, PBS droplets form multiple crystals (Fig. 2d; also Fig. S4c) as the droplet rapidly dries, with multiple nucleation events occurring as the solute concentration surpasses critical supersaturation for efflorescence (41).

The rapid changes in particle size and water content during drying lead to conditions in the aerosol phase that are not accessible in the bulk liquid (e.g., supersaturated solute, high salt concentrations, ultraviscous and even glassy states) for nearly all ambient conditions when the RH falls below 70%, potentially impacting the longevity of enclosed microorganisms (28, 42–45). In Fig. 2e and f, the time-dependent changes in solute concentrations accompanying the evaporation of nonmetabolized LB broth and PBS droplets into gas phases with 30, 50, 70, and 90% RHs are compared. The dynamics for these solution droplets are simulated using a quasisteady evaporation model that accounts for the interplay of mass and heat transport during drying and is benchmarked against the experimental measurements (46).

The impacts on *E. coli* MRE162 survival of the interconnected changes in size, particle morphology, and solute concentrations taking place during the evaporation of PBS and LB broth droplets at 300 s are reported in Fig. 2g and h. Bacterial survival is reported as the ability of a bacterium to form a colony (expressed in CFU) after suspension, collection, and 24 h of incubation. Overall, an inverse correlation between the final equilibrated solute concentration and *E. coli* MRE162 survival is observed.

At high RHs (90 to 70%), where all droplets remain homogeneous during evaporation for both droplet compositions, bacterial survival in LB broth droplets shows a significant decrease as the RH decreases, potentially due to the high solute concentration at 70% RH. In the case of PBS droplet composition, the reduction in survival with RH reduction is moderate. Higher survival at 70% RH (Fig. 2h) is reported in PBS droplets, possibly due to the higher mass of water, larger droplet size, and lower solute concentration found when equilibrium with the gas-phase composition is achieved (cf. Fig. S6 and S7).

Under the driest conditions (50% to 30% RH), a significant decline in *E. coli* MRE162 survival is observed in PBS droplets (Fig. 2h), compared with a smaller decrease for LB broth droplets (Fig. 2g). This sudden reduction in survival in PBS coincides with a transition in particle phase, in this case from homogeneous droplets to salt crystals (Fig. 2b and d). When droplet compositions were compared, a statistically significant difference in survival was observed at 50% RH, also matching the difference in droplet morphology between compositions, showing lower survivability in LB broth droplets, where inclusions were observed, in contrast with the homogeneity of PBS droplets (compare Fig. 2a and b). Conversely, the survival reported in LB broth droplets at 30% RH is marginally higher than that in PBS droplets, likely due to the presence of organic components in LB broth, which potentially enhance survival (compare Fig. 2g and h).

**No loss of viability is observed during the rapid drying phase of bioaerosol droplets; bacteria act as crystallization nuclei.** Time-dependent measurements of the viability of *E. coli* MRE162 enclosed in LB broth and PBS droplets equilibrated at various RHs were performed over 1 h (Fig. 3). Due to the gentle aerosolization processes and high-resolution sampling achieved with CELEBS, the CFU observed for the shortest survival measurements (suspension time, $<5$ s) agree with the estimated microbial concentrations in the droplets. This expected concentration is estimated from the cell concentration in the suspension loaded into the droplet-on-demand (DoD) generator, described by a Gaussian distribution when concentrations are in the order of $10^8$ cells $ml^{-1}$. The efficiency of the sequence of processes (from biological sample solution to aerosol droplet creation to aerosol droplet sampling/recovery) has been discussed in detail in our previous work (25). Thus, only the biological decay processes occurring in the aerosol phase need be considered.

Little decline in biological viability over a timescale of 5 s is observed for any of the droplet compositions and RHs. This holds even for the very rapid evaporation and

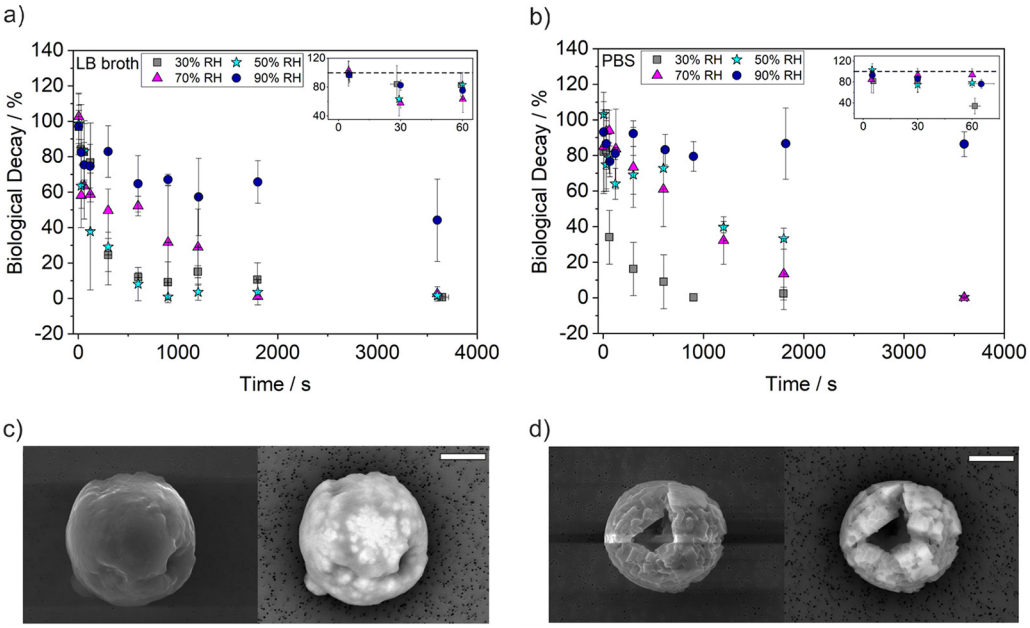


**FIG 3** (a and b) Relationship between solute composition and the survival of airborne bacteria as a function of RH. The survival of *E. coli* MRE162 [$(2.6 \pm 0.6) \times 10^8$ CFU ml$^{-1}$] in LB broth (a) and PBS (b) droplets is shown. Note that in panel b, the data points for 50% and 70% RH at 3,600 s overlap. (Inset) Survival decay during a time frame of 60 s of levitation. (c and d) SEM and backscattered electron images for LB broth (c) and PBS (d) droplets containing *E. coli* MRE162 at $(2.6 \pm 0.6) \times 10^9$ CFU ml$^{-1}$ at 30% RH. Bars, 5 $\mu$m.

equilibration time at the lowest RHs (as shown, e.g., in Fig. S6a and S7a), where the evaporative cooling and rise in solute concentration at the droplet surface can be expected to be most severe. Thus, the dynamic processes taking place (e.g., water evaporation, surface cooling, rapid changes in size and solute composition) seem not to immediately impact *E. coli* MRE162 survival. The lack of impact of the dynamics occurring during evaporation can be contrasted with current assumptions whereby two different decay constants have been reported, suggested as arising from a rapid initial decay attributed to the drying process and a subsequent slower secondary phase associated with oxidative stress and the effect of environmental conditions (11–13, 47–50). These studies were performed by using reflux atomization for aerosol generation and various methodologies, such as the rotating drum and static and dynamic storage chambers, for particle suspension (11, 13, 47, 48, 50).

The marginal decay observed up to 5 s (Fig. 3a and b) suggests that the rapid initial loss of viability (with decay constants of 1 s) reported previously (13, 48) is likely not occurring in the aerosol phase but may be a systematic artifact of the aerosolization process used, since many aerosol generators impact the structural integrity of microorganisms when they are nebulized (22, 23). Further, the disturbance in gas-phase conditions produced by the cumulative mass of water introduced into the system by the cloud of droplets from nebulizers is often not considered, and therefore, the conditions studied often are not precisely reported during droplet evaporation (tens of minutes may be necessary for the droplet cloud to reach equilibrium) (51). The ability to determine microbial decay during dynamic microphysical processes in the aerosol phase is unique to TAMBAS.

The time for the first decay is apparent in Fig. 3 and is considerably longer that the time required for the droplets to reach thermodynamic equilibrium, a time that is dependent on RH. Interestingly, a significant decrease in the viability of airborne bacteria (compared to the 5-s measurement) is observed only at the lowest RHs (30 and 50%) for droplets composed of PBS during the first 60 s of suspension (*P* values, 0.00004 and 0.00015, respectively). In contrast, the loss of viability was significant only at the highest RHs (70 and 90%) (*P* values, 0.0013 and 0.0001, respectively) in the case of LB

broth droplets. This general trend describing greater survivability in PBS droplets at high RHs is maintained at longer timescales. Thus, no significant decay is observed at 90% RH after 1-h suspensions for droplets composed of PBS ($P$, 0.2), while the reduction in viability is significant for droplets composed of LB broth ($P$, 0.00005). This divergence in survival in droplets of different compositions may be a result of the higher solute hygroscopicity of PBS, linked to greater water content in the droplets and lower solute concentrations (compare Fig. S6b and S7b).

Interestingly, the structure of bacterium-containing PBS particles dried at 30% RH observed in the SEM analysis shows *E. coli* MRE162 cells embedded in the salt crystals, coinciding with a considerable increase in the overall number of crystals compared with that for pure PBS droplets (compare Fig. 2d with Fig. 3d and Fig. S4c with Fig. S4d), in agreement with the notion that bacteria act as crystallization nuclei. Conversely, little change in the phase behavior of LB broth is observed when the particles contain bacteria (compare Fig. 2c with Fig. 3c and Fig. S4a with Fig. S4b).

**Droplet size affects the viability of airborne bacteria.** To isolate the effects of different factors (such as solute concentration and droplet size) impacting the survival of airborne bacteria, the viability responses of *E. coli* MRE162 levitated for 300 s in droplets of LB broth with different initial solute concentrations equilibrating at 50% RH are compared in Fig. 4c. The evaporation profiles of nonmetabolized LB broth with three different starting concentrations are reported in Fig. 4a. The different initial concentrations lead to different equilibrated sizes, although all the droplets achieve the same concentration of LB broth and moisture content when reaching an equilibrium at a specific RH (Fig. 4b), and thereby all have the same density. Thus, evaluation of the effect solely of different particle sizes containing the same solute concentration at equilibrium is possible. This is a unique and important element of this approach. The data in Fig. 4c suggest that either particle size or the dynamic processes during evaporation, or both, play a crucial role in the survival response of *E. coli* MRE162.

## DISCUSSION

The novel approach presented here, TAMBAS, provides an opportunity to explore the effect of individual parameters on the survival of airborne microorganisms, which could be crucial for fully understanding the fundamental mechanisms that control the transmission of airborne diseases. The ability to measure the impact of aerosol dynamics on the survival of microorganisms in the aerosol phase while reducing the stresses involved in the generation, suspension, and sampling processes is unique to this technique. Previous studies performed with evaporating sessile droplets (i.e., droplets deposited on surfaces) (52) or conventional technologies (20, 53) often were not representative of the natural mechanisms involved in the airborne transmission of disease. Therefore, data comparison becomes challenging due to the wide variety of methodologies, bioaerosol compositions, and environmental conditions employed in longevity studies.

Figure S9 in the supplemental material shows the viability of *E. coli* MRE162 at 300 s of suspension as a function of six different parameters (droplet cooling, volume reduction, surface-to-volume ratio, NaCl concentration, solute concentration, and droplet volume), where only three (Fig. S9a, b, and e) demonstrate a large collective correlation for both particle types (PBS and LB broth), with $R^2$ values of 0.78, 0.80, and 0.87 for droplet cooling, volume reduction, and solute concentration, respectively. These correlations of viability with droplet cooling, volume reduction, and solute concentration are all associated with the initial water mass flux from the droplet at the point of generation. Thus, although there is no apparent loss in viability during the drying phase (the first 5 to 10 s), the impact of the initial mass flux from the droplet on microbe longevity, and the overall change in size (Fig. 4), are consistent with an impact on viability over longer timescales. Put simply, the data suggest that the initial evaporation dynamics of the bioaerosol have a pronounced and predictable delayed effect on bioaerosol longevity and should be further explored. Ultimately, this transformative approach will contribute to a more complete understanding of the funda-

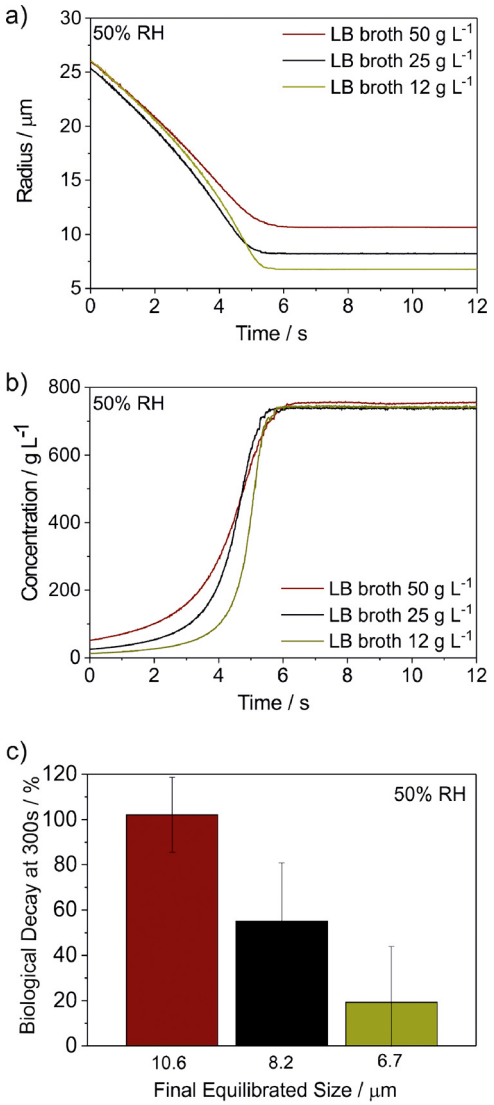


**FIG 4** (a and b) Comparison of the measured particle radii (a) and changes in solute concentration (in grams per liter) (b) of LB broth droplets with different initial solute concentrations (50, 25, or 12 g/liter [represented by red, dark blue, or chartreuse lines, respectively]) evaporating at 50% RH and 20°C. (c) Effect of the equilibrium particle size on bacterial viability. All the survivability data are expressed as the averages and standard deviations for three replicates per experiment where populations from 2 to 6 droplets were levitated.

mental factors influencing the airborne transmission of pathogens, enabling the development of refined hazard mitigation strategies.

## MATERIALS AND METHODS

To demonstrate the utility of the new approach, *E. coli* MRE162 was chosen as both a benchmark and a representative system for the study of bioaerosols. This bacterial strain presents a higher aerosol stability than other Gram-negative bacteria and has been proposed previously as a simulant for respiratory pathogens and as a model for understanding the effect of "outdoor" conditions on survival (54–58). In addition, wastewater treatment plants (WWTP) are a major source of bioaerosol emissions due to mechanical sewage treatment devices. *E. coli* has been detected in air sampled around such facilities and is known to cause zoonotic infections via the aerosol route (59).

**Comprehensive methodology for bioaerosol survival studies.** TAMBAS was developed to elucidate the fundamental mechanisms responsible for degrading the viability of airborne microorganisms and thus to identify the parameters that define the transmission of airborne infection. The complementarity of two methodologies is used to resolve the complex interrelationship between the physicochemical and biological processes taking place from the production mechanism, such as coughing and sneezing (60), until the droplet reaches equilibrium and through to rehydration during the inhalation

process. The CK-EDB method can be used to study the evaporation/condensation kinetics, the solute hygroscopic properties, and the evolving particle morphology during the drying of single levitated aerosol particles (37). These data can be used to develop a detailed understanding of the thermodynamic and kinetic processes that take place during the evaporation and condensation cycle occurring in a droplet life span. Additionally, with the novel CELEBS method, the survival rates of microorganisms in populations of bioaerosol droplets can be determined as a function of atmospheric conditions, biological and chemical composition, and other biological factors, such as the microbial concentration and physiology (25). An overview of both methodologies is included in Table S1 in the supplemental material. Some of the key features accessible with this technique, enabling a detailed analysis of biological decay as a function of time, are the suspension of particles in the true airborne state under a regulated atmosphere for a well-defined and unlimited period (~3 s to days) and with high time resolution (<1 s); probing of a quantifiable number of individual-microbe-containing droplets in each experiment; and control over the number of microbial cells hosted within each droplet. Importantly, the key elements of this methodology (e.g., the use of droplet-on-demand [DoD] generation to produce droplets of tailored composition, the imposition of low levels of charge on the particles to levitate them) do not impact the viability of the microorganisms (25). The setup, operation, and data analysis of both methodologies are described in detail below and in Fig. S1 and S2.

Unique to this comprehensive methodology is the ability to combine our understanding of microphysics and microbiology in the airborne state with time resolutions of 10 ms and 1 s, respectively. Not only is there an opportunity to achieve this in the aerosol phase, but the methodology allows us to investigate repeatability and reproducibility for many droplets under the same desired initial conditions while minimizing stresses affecting microbial viability during aerosolization, leading to low experimental uncertainties. This valuable alternative to conventional technologies will allow researchers to develop more-accurate strategies to control the airborne transmission of disease.

**Comparative kinetics methodology for physicochemical characterization of bioaerosols.** The ability to measure the dynamic behavior of single levitated droplets using the concentric cylindrical electrodynamic balance (EDB) has been discussed in the literature (27). A sample solution of known chemical and biological composition is introduced into the reservoir of a DoD microdispenser (MJ-ABP-01; orifice, 30 $\mu$m; MicroFab). Single droplets are generated with a high level of size reproducibility (Fig. S5) by applying a pulse voltage to the piezoelectric tip of the DoD microdispenser, and a small net charge is induced during droplet formation by employing a high-voltage induction electrode located 2 to 3 mm from the tip of the DoD microdispenser, allowing the droplet to be manipulated in the EDB. Approximately 100 ms after generation, the droplet is confined in the null point of the electrodynamic field, where a 200-ml/min gas inlet at a temperature of 20°C regulates the RH (from 10% to 90%) inside the CK-EDB chamber by altering the mixing ratio of humidified and dry nitrogen flows. The trapped droplet is illuminated by a laser beam (ventus Continuous Wave [CW] laser; Laser Quantum) with a wavelength ($\lambda$) of 532 nm, and a charge-coupled device (CCD) camera (Thorlabs) records the light-scattering pattern, referred to as "phase function," at a central viewing angle of 45° every ~10 ms. By using geometric optics approximation, the angular separation between light-scattering fringes ($\Delta\theta$) in the phase function pattern is used to determine the absolute radius of the droplet (27) as a function of time together with the droplet morphology (37). The droplet radius is estimated from the expression

$$r = \frac{\lambda}{\Delta\theta}\left(\cos\left(\frac{\theta}{2}\right) + \frac{n\sin\left(\frac{\theta}{2}\right)}{\sqrt{1+n^2-2n\cos\left(\frac{\theta}{2}\right)}}\right)^{-1} \quad (1)$$

where $r$ is the radius of the droplet, $\theta$ is the central viewing angle, and $n$ is the droplet refractive index (RI), which is initially set as a constant value (61). In a postanalysis process, the variation in the droplet RI with the mass fraction of solute (mfs) during evaporation is accounted for by applying a solute RI parametrization generated by using the molar refraction mixing rule (62). This revision process is repeated over 2 to 3 iterations until the radii and corresponding RI values converge, providing accurate data for the droplet radius (29).

From the droplet evaporation measurements, the hygroscopic growth properties at thermodynamic equilibrium can be retrieved by using a comparative kinetics approach described in the literature and the section below (29). Finally, the hygroscopicity data derived from the above process can be used to predict the evaporation dynamics for droplets of any size, composition, gas-phase RH, and temperature (26).

**(i) Determination of droplet hygroscopicity properties.** A comparative kinetics approach described in previous publications is used to retrieve the hygroscopic equilibrium response of solution droplets (27, 37, 63). Specifically, sequences of 10 pairs of probe and sample droplets with different chemical compositions are sequentially dispensed by two DoD microdispensers. First, the evaporation profile of a probe droplet (in well-known systems such as water or aqueous NaCl solutions) is used to accurately determine the RH of the trapping atmosphere. Second, measurements of the corrected radius of the sample droplet over time are converted into mass by using a density parametrization. From these data, the mass flux as a function of time is calculated and used to determine the water activity at the droplet surface by using the mass and heat transport equation of Kulmala et al. (46). Finally, the droplet hygroscopicity is represented as the variation in mfs (calculated from the initial size and droplet composition) against the variation in water activity, providing the whole hygroscopicity curve.

**(ii) Simulations of droplet evaporation kinetics.** Once the hygroscopic properties of the sample droplet are determined, it is possible to develop solute hygroscopicity parametrization by using the

equation developed by Kreidenweis et al. (64), which is then introduced into the Kulmala model together with the density treatment of the solution droplet to generate predictions of mass transfer kinetics for any initial solute concentration, droplet size, and gas-phase RH and temperature. Simulations resulting from this approach have shown excellent agreement with experimental data. Errors associated with the thermodynamic predictions have also been discussed in previous work (26).The possibility of building models that enable prediction of the evaporation kinetics of aerosol droplets containing microorganisms as a function of the initial droplet radius and composition allows further exploration of the interplay between all the physiochemical parameters affecting the survival of airborne bacteria (Fig. S8).

**(iii) Inferring particle morphology from the light-scattering pattern.** The same light-scattering pattern employed in the estimation of droplet size has also been used to qualitatively infer the morphology of single levitated particles (65, 66). Based on qualitative characteristics of the phase function, a new semiquantitative methodology to differentiate among four main particle structures has been developed recently (37). This robust approach relies on more than 1 million observations of individual light-scattering patterns to develop an algorithm that categorizes the particle morphology as homogeneous, a core-shell structure, an inclusion-containing particle, or a crystal or inhomogeneous particle. Specifically, a homogeneous, spherical evaporating droplet produces a regular and smooth evolution in its light-scattering pattern, which is characterized by equally spaced peaks. In the case of droplets containing inclusions, the regularity in the space between the peaks is maintained; however, the intensity pattern can be randomly enhanced or reduced depending on the location of the inclusions within the droplet volume. In the evaporation of a droplet containing inclusions, the absolute number of inclusions remains constant and is determined based on the initial concentration pipetted in the DoD generator. However, the concentration of inclusions increases over time as water evaporates. The sensitivity of this method for the detection of inclusions within a particle is determined by their concentration. The absolute number of inclusions and their sizes have been shown to be irrelevant to the determination of the lower detection limit (37). The phase function for droplets within a concentration gradient or core-shell structure is characterized by an additional envelope of intensity modulation superimposed on the regular fringes observed from a spherical particle due to the presence of a secondary structure. Finally, irregular or crystal particles exhibit a highly irregular phase function over time, which makes determination of the particle size impossible. The sphere-equivalent size can be inferred from the size and solute concentration of the initial droplet. The ability to detect different morphologies on an individual bioaerosol droplet allows the possibility of exploring the impact of particle phase and structure on microbial viability.

**Levitation and sampling methodology for biophysical characterization of bioaerosols.** The ability to determine the biological decay rates of bioaerosols as a function of time, atmospheric conditions, and chemical and biological composition has been developed recently (25). The CELEBS apparatus is an adaptation of the double-ring electrodynamic trap (EDT) (67) with important modifications that enable the generation, levitation, and sampling of populations of bioaerosol droplets while minimizing the stresses associated with these processes when conventional techniques are used for bioaerosol studies (68, 69). All components are enclosed in a 3-dimensional (3D) printed chamber to avoid disturbance of the levitated particles in a conditioned environment. CELEBS utilizes the same method of droplet generation used in the CK-EDB, with the difference that in this case, a population of droplets is generated. A high-voltage induction electrode induces a small net charge on each particle, allowing the population of droplets to be trapped in the electrodynamic field generated by applying an AC voltage (1,000 to 2,700 V) to the two parallel ring electrodes located in the center of the chamber. The net like charge on all particles prevents coalescence among the population of droplets. The particles are confined in the electrodynamic field with a gas inlet, which enables control of the atmospheric conditions (i.e., temperature, RH, gas, etc.) inside the chamber, and a 580-nm LED light illuminates the population of droplets, allowing particle enumeration by using a LabView program developed in-house. A probe connected to the gas inlet registers the RH percentage and temperature to which the droplets are exposed at every time. After the desired levitation period, the shielding on the sampling area is removed by retracting a safety plate. Then the particles are extracted from the EDT onto the substrate holder by gradually reducing the amplitude of the waveform applied to the electrodes. The CELEBS instrument provides 100% efficiency in the collection of the levitated particles by utilizing sampling velocities similar to those used with electrostatic precipitators (70), reducing the stresses associated with conventional bioaerosol samplers such as impingers (24, 71). In addition, this methodology presents the possibility of probing viability/infectivity in any type of substrate (i.e., lung cells, microbiological media, ATP assays, etc.). In this work, the bioaerosol droplets were sampled on petri dishes containing a ~3-mm layer of LB agar and a 300-$\mu$l volume of LB broth located in the center of the plate. Finally, the petri dishes were removed from the instrument, the LB broth containing the sampled bioaerosol was spread over the agar surface, and the plates were incubated for 24 h at 37°C. The approach used to calculate the survival rates of bacteria was described by us previously (25) and is also included in the supplemental material.

**Measurements of survival rate.** The characterization of bioaerosol survival rates has been described in our previous work (25). The loss of viability of airborne pathogens is represented as a reduction in their ability to form colonies on plating media (culturability) as a function of time in the aerosol phase by using the following equation:

$$\mathrm{BD} = \frac{C_{\mathrm{culturable}}(\mathrm{TEST})}{C_{\mathrm{culturable}}(\mathrm{CONTROL})} \times 100 \qquad (2)$$

where BD is biological decay and $C_{\mathrm{culturable}}$ (TEST) is the number of CFU obtained after the incubation of

the bioaerosol population that was levitated for a set time interval. This measurement is normalized by using a $C_{culturable}$ (CONTROL) measurement to facilitate data comparison. Two options are valid as control measurements. One is the absolute number of bacterial cells contained in the droplets, estimated from the bacterial concentration introduced into the DoD generator. The second option is to measure the number of culturable cells (CFU per droplet) obtained after a levitation time under 7 s in a preceding measurement. In this case, the levitation period is too brief to impact the viability of the microorganisms and is therefore considered a nonexposure measurement. The validity of this assumption has been confirmed by comparing a series of CFU counts per droplet obtained after 5-s "harmless" levitations with the original CFU count per droplet, estimated by using the concentration of the cell suspension pipetted in the DoD generator (25).

## SUPPLEMENTAL MATERIAL

Supplemental material is available online only.

**SUPPLEMENTAL FILE 1**, PDF file, 1.5 MB.

## ACKNOWLEDGMENTS

We acknowledge the contribution of the Natural Environment Research Council (NCAS-NERC) and the Defence Science and Technology Laboratory (Dstl) for financial support through studentship funding. R.J.T. recognizes funding contributed by the UK Ministry of Defence.

We acknowledge Jean-Charles Eloi, electron microscopy technician in the School of Chemistry at the University of Bristol, for his contribution in acquiring the SEM images used in this study.

A.E.H. and M.O.F. developed the approach with support from J.P.R., R.J.T., and H.O. A.E.H. and J.P.R. conceived and designed the project. M.O.F. carried out the data analysis, wrote the paper, assisted in the design and development of the methodology, and performed the laboratory work with support from A.E.H., R.J.T., and H.O. A.E.H. and J.P.R. are joint corresponding authors, supervised and coordinated the research, and edited the manuscript for publication. J.P.R. acquired funding and administered the project.

We declare that we have no conflicts of interest.

## REFERENCES

1. Stilianakis NI, Drossinos Y. 2010. Dynamics of infectious disease transmission by inhalable respiratory droplets. J R Soc Interface 7:1355–1366. https://doi.org/10.1098/rsif.2010.0026.
2. Han ZY, Weng WG, Huang QY. 2013. Characterizations of particle size distribution of the droplets exhaled by sneeze. J R Soc Interface 10: 20130560. https://doi.org/10.1098/rsif.2013.0560.
3. Sze To GN, Wan MP, Chao CYH, Fang L, Melikov A. 2009. Experimental study of dispersion and deposition of expiratory aerosols in aircraft cabins and impact on infectious disease transmission. Aerosol Sci Technol 43:466–485. https://doi.org/10.1080/02786820902736658.
4. Wan MP, Sze To GN, Chao CYH, Wan MP, Fang L, Melikov A. 2009. Modeling the fate of expiratory aerosols and the associated infection risk in an aircraft cabin environment. Aerosol Sci Technol 43:322–343. https://doi.org/10.1080/02786820802641461.
5. Douwes J, Thorne P, Pearce N, Heederik D. 2003. Bioaerosol health effects and exposure assessment: progress and prospects. Ann Occup Hyg 47:187–200. https://doi.org/10.1093/annhyg/meg032.
6. Morawska L, Cao J. 2020. Airborne transmission of SARS-CoV-2: the world should face the reality. Environ Int 139:105730. https://doi.org/10.1016/j.envint.2020.105730.
7. Haddrell AE, Thomas RJ. 2017. Aerobiology: experimental considerations, observations, and future tools. Appl Environ Microbiol 83:e00809-17. https://doi.org/10.1128/AEM.00809-17.
8. Marr LC, Tang JW, Van Mullekom J, Lakdawala SS. 2019. Mechanistic insights into the effect of humidity on airborne influenza virus survival, transmission and incidence. J R Soc Interface 16:20180298. https://doi.org/10.1098/rsif.2018.0298.
9. Kukavica-Ibrulj I, Levesque RC. 2008. Animal models of chronic lung infection with Pseudomonas aeruginosa: useful tools for cystic fibrosis studies. Lab Anim 42:389–412. https://doi.org/10.1258/la.2007.06014e.
10. Du P, Du R, Ren W, Lu Z, Fu P. 2018. Seasonal variation characteristic of inhalable microbial communities in PM 2.5 in Beijing city, China. Sci Total Environ 610–611:308–315. https://doi.org/10.1016/j.scitotenv.2017.07.097.
11. Dunklin EW, Puck TT. 1948. The lethal effect of relative humidity on airborne bacteria. J Exp Med 87:87–101. https://doi.org/10.1084/jem.87.2.87.
12. Benbough JE. 1967. Death mechanisms in airborne Escherichia coli. J Gen Microbiol 47:325–333. https://doi.org/10.1099/00221287-47-3-325.
13. Webb SJ. 1959. Factors affecting the viability of air-borne bacteria. Can J Microbiol 14:742–745.
14. Lighthart B, Shaffer BT. 1997. Increased airborne bacterial survival as a function of particle content and size. Aerosol Sci Technol 27:439–446. https://doi.org/10.1080/02786829708965483.
15. Jones AM, Harrison RM. 2004. The effects of meteorological factors on atmospheric bioaerosol concentrations. A review. Sci Total Environ 326: 151–180. https://doi.org/10.1016/j.scitotenv.2003.11.021.
16. Davis MS, Bateman JB. 1960. Relative humidity and the killing of bacteria. I. Observations on Escherichia coli and Micrococcus lysodeikticus. J Bacteriol 80:577–579. https://doi.org/10.1128/JB.80.5.577-579.1960.
17. Cox CS, Goldberg LJ. 1972. Aerosol survival of Pasteurella tularensis and the influence of relative humidity. Appl Microbiol 23:1–3. https://doi.org/10.1128/AEM.23.1.1-3.1972.
18. Benbough JE. 1971. Some factors affecting the survival of airborne viruses. J Gen Virol 10:209–220. https://doi.org/10.1099/0022-1317-10-3-209.
19. Ehrlich R, Miller S, Walker RL. 1970. Relationship between atmospheric temperature and survival of airborne bacteria. Appl Microbiol 19: 245–249. https://doi.org/10.1128/AEM.19.2.245-249.1970.
20. Fernstrom A, Goldblatt M. 2013. Aerobiology and its role in the transmission of infectious diseases. J Pathog 2013:493960. https://doi.org/10.1155/2013/493960.
21. Gralton J, Tovey E, McLaws ML, Rawlinson WD. 2011. The role of particle size in aerosolised pathogen transmission: a review. J Infect 62:1–13. https://doi.org/10.1016/j.jinf.2010.11.010.
22. Alsved M, Bourouiba L, Duchaine C, Löndahl J, Marr LC, Parker ST, Prussin AJ, Thomas RJ. 2020. Natural sources and experimental generation of

bioaerosols: challenges and perspectives. Aerosol Sci Technol 54:547–571. https://doi.org/10.1080/02786826.2019.1682509.
23. Zhen H, Han T, Fennell DE, Mainelis G. 2014. A systematic comparison of four bioaerosol generators: effect on culturability and cell membrane integrity when aerosolizing Escherichia coli bacteria. J Aerosol Sci 70:67–79. https://doi.org/10.1016/j.jaerosci.2014.01.002.
24. Dabisch P, Bower K, Dorsey B, Wronka L. 2012. Recovery efficiencies for Burkholderia thailandensis from various aerosol sampling media. Front Cell Infect Microbiol 2:78. https://doi.org/10.3389/fcimb.2012.00078.
25. Otero-Fernandez M, Thomas RJ, Garton NJ, Hudson A, Haddrell A, Reid JP. 2019. Assessing the airborne survival of bacteria in populations of aerosol droplets with a novel technology. J R Soc Interface 16:20180779. https://doi.org/10.1098/rsif.2018.0779.
26. Davies JF, Haddrell AE, Rickards AMJ, Reid JP. 2013. Simultaneous analysis of the equilibrium hygroscopicity and water transport kinetics of liquid aerosol. Anal Chem 85:5819–5826. https://doi.org/10.1021/ac4005502.
27. Davies JF, Haddrell AE, Reid JP. 2012. Time-resolved measurements of the evaporation of volatile components from single aerosol droplets. Aerosol Sci Technol 46:666–677. https://doi.org/10.1080/02786826.2011.652750.
28. Power RM, Simpson SH, Reid JP, Hudson AJ. 2013. The transition from liquid to solid-like behaviour in ultrahigh viscosity aerosol particles. Chem Sci 4:2597. https://doi.org/10.1039/c3sc50682g.
29. Rovelli G, Miles REH, Reid JP, Clegg SL. 2016. Accurate measurements of aerosol hygroscopic growth over a wide range in relative humidity. J Phys Chem A 120:4376–4388. https://doi.org/10.1021/acs.jpca.6b04194.
30. Carslaw KS, Clegg SL, Brimblecombe P. 1995. A thermodynamic model of the system HCl-$HNO_3$-$H_2SO_4$-$H_2O$, including solubilities of HBr, from $<$200 to 328 K. J Phys Chem 99:11557–11574. https://doi.org/10.1021/j100029a039.
31. Goldberg LJ, Watkins HMS, Boerke EE, Chatigny MA. 1958. The use of a rotating drum for the study of aerosols over extended periods of time. Am J Hyg 68:85–93. https://doi.org/10.1093/oxfordjournals.aje.a119954.
32. Cox CS, Gagen SJ, Baxter J. 1974. Aerosol survival of Serratia marcescens as a function of oxygen concentration, relative humidity, and time. Can J Microbiol 20:1529–1534. https://doi.org/10.1139/m74-239.
33. Cox CS. 1971. Aerosol survival of Pasteurella tularensis disseminated from the wet and dry states. Appl Microbiol 21:482–486. https://doi.org/10.1128/AEM.21.3.482-486.1971.
34. Donaldson AI, Ferris NP. 1975. The survival of foot-and-mouth disease virus in open air conditions. J Hyg (Lond) 74:409–416. https://doi.org/10.1017/s002217240004691x.
35. Lever MS, Williams A, Bennett AM. 2000. Survival of mycobacterial species in aerosols generated from artificial saliva. Lett Appl Microbiol 31:238–241. https://doi.org/10.1046/j.1365-2672.2000.00807.x.
36. Zuo Z, Kuehn TH, Bekele AZ, Mor SK, Verma H, Goyal SM, Raynor PC, Pui DYH. 2014. Survival of airborne MS2 bacteriophage generated from human saliva, artificial saliva, and cell culture medium. Appl Environ Microbiol 80:2796–2803. https://doi.org/10.1128/AEM.00056-14.
37. Haddrell A, Rovelli G, Lewis D, Church T, Reid J. 2019. Identifying time-dependent changes in the morphology of an individual aerosol particle from its light scattering pattern. Aerosol Sci Technol 53:1334–1351. https://doi.org/10.1080/02786826.2019.1661351.
38. Davies JF, Haddrell AE, Miles REH, Bull CR, Reid JP. 2012. Bulk, surface, and gas-phase limited water transport in aerosol. J Phys Chem A 116:10987–10998. https://doi.org/10.1021/jp3086667.
39. Bones DL, Reid JP, Lienhard DM, Krieger UK. 2012. Comparing the mechanism of water condensation and evaporation in glassy aerosol. Proc Natl Acad Sci U S A 109:11613–11618. https://doi.org/10.1073/pnas.1200691109.
40. Goto M, Oaki Y, Imai H. 2016. Dendritic growth of NaCl crystals in a gel matrix: variation of branching and control of bending. Cryst Growth Des 16:4278–4284. https://doi.org/10.1021/acs.cgd.6b00323.
41. Gregson FKA, Robinson JF, Miles REH, Royall CP, Reid JP. 2019. Drying kinetics of salt solution droplets: water evaporation rates and crystallization. J Phys Chem B 123:266–276. https://doi.org/10.1021/acs.jpcb.8b09584.
42. Yang W, Marr LC. 2012. Mechanisms by which ambient humidity may affect viruses in aerosols. Appl Environ Microbiol 78:6781–6788. https://doi.org/10.1128/AEM.01658-12.
43. Haddrell AE, Hargreaves G, Davies JF, Reid JP. 2013. Control over hygroscopic growth of saline aqueous aerosol using Pluronic polymer additives. Int J Pharm 443:183–192. https://doi.org/10.1016/j.ijpharm.2012.12.039.
44. Power RM, Reid JP. 2014. Probing the micro-rheological properties of aerosol particles using optical tweezers. Rep Prog Phys 77:074601. https://doi.org/10.1088/0034-4885/77/7/074601.
45. Girod M, Moyano E, Campbell DI, Cooks RG. 2011. Accelerated bimolecular reactions in microdroplets studied by desorption electrospray ionization mass spectrometry. Chem Sci 2:501–510. https://doi.org/10.1039/C0SC00416B.
46. Kulmala M, Vesala T, Wagner PE. 1993. An analytical expression for the rate of binary condensational particle growth. Proc R Soc A Math Phys Eng Sci 441:589–605.
47. Ferry RM, Brown WF, Damon EB. 1958. Studies of the loss of viability of bacterial aerosols. III. Factors affecting death rates of certain non-pathogens. J Hyg (Lond) 56:389–403. https://doi.org/10.1017/s0022172400037888.
48. Ferry RM, Brown WF, Damon EB. 1958. Studies of the loss of viability of stored bacterial aerosols. II. Death rates of several non-pathogenic organisms in relation to biological and structural characteristics. J Hyg (Lond) 56:125–150. https://doi.org/10.1017/s002217240003761x.
49. Scott WJ. 1958. The effect of residual water on the survival of dried bacteria during storage. J Gen Microbiol 19:624–633. https://doi.org/10.1099/00221287-19-3-624.
50. Ferry RM, Maple TG. 1954. Studies of the loss of viability of stored bacterial aerosols. I. Micrococcus candidus. J Infect Dis 95:142–159. https://doi.org/10.1093/infdis/95.2.142.
51. Cai C, Stewart DJ, Reid JP, Zhang YH, Ohm P, Dutcher CS, Clegg SL. 2015. Organic component vapor pressures and hygroscopicities of aqueous aerosol measured by optical tweezers. J Phys Chem A 119:704–718. https://doi.org/10.1021/jp510525r.
52. Vejerano EP, Marr LC. 2018. Physico-chemical characteristics of evaporating respiratory fluid droplets. J R Soc Interface 15:20170939. https://doi.org/10.1098/rsif.2017.0939.
53. Willem L, van Kerckhove K, Chao DL, Hens N, Beutels P. 2012. A nice day for an infection? Weather conditions and social contact patterns relevant to influenza transmission. PLoS One 7:e48695. https://doi.org/10.1371/journal.pone.0048695.
54. Ng TW, Chan WL, Lai KM. 2017. Importance of stress-response genes to the survival of airborne Escherichia coli under different levels of relative humidity. AMB Express 7:71. https://doi.org/10.1186/s13568-017-0376-3.
55. Lin K, Marr LC. 2020. Humidity-dependent decay of viruses, but not bacteria, in aerosols and droplets follows disinfection kinetics. Environ Sci Technol 54:1024–1032. https://doi.org/10.1021/acs.est.9b04959.
56. Dybwad M, Skogan G. 2017. Aerobiological stabilities of different cell clusters of different compositions. Appl Environ Microbiol 83:e0823-17. https://doi.org/10.1128/AEM.00823-17.
57. de Mik G, de Groot I. 1977. The germicidal effect of the open air in different parts of The Netherlands. J Hyg (Lond) 78:175–187. https://doi.org/10.1017/s0022172400056072.
58. Benbough JE, Hambleton P, Martin KL, Strange RE. 1972. Effect of aerosolization on the transport of -methyl glucoside and galactosides into Escherichia coli. J Gen Microbiol 72:511–520. https://doi.org/10.1099/00221287-72-3-511.
59. Vantarakis A, Paparrodopoulos S, Kokkinos P, Vantarakis G, Fragou K, Detorakis I. 2016. Impact on the quality of life when living close to a municipal wastewater treatment plant. J Environ Public Health 2016:8467023. https://doi.org/10.1155/2016/8467023.
60. Johnson GR, Morawska L, Ristovski ZD, Hargreaves M, Mengersen K, Chao CYH, Wan MP, Li Y, Xie X, Katoshevski D, Corbett S. 2011. Modality of human expired aerosol size distributions. J Aerosol Sci 42:839–851. https://doi.org/10.1016/j.jaerosci.2011.07.009.
61. Glantschnig WJ, Chen S-H. 1981. Light scattering from water droplets in the geometrical optics approximation. Appl Opt 20:2499–2509. https://doi.org/10.1364/AO.20.002499.
62. Cai C, Miles REH, Cotterell MI, Marsh A, Rovelli G, Rickards AMJ, Zhang Y-H, Reid JP. 2016. Comparison of methods for predicting the compositional dependence of the density and refractive index of organic-aqueous aerosols. J Phys Chem A 120:6604–6617. https://doi.org/10.1021/acs.jpca.6b05986.
63. Rovelli G, Miles EHR, Reid PJ, Clegg LS. 2017. Hygroscopic properties of aminium sulfate aerosols. Atmos Chem Phys 17:4369–4385. https://doi.org/10.5194/acp-17-4369-2017.

64. Kreidenweis SM, Koehler K, DeMott PJ, Prenni AJ, Carrico C, Ervens B. 2005. Water activity and activation diameters from hygroscopicity data. Part I. Theory and application to inorganic salts. Atmos Chem Phys 5:1357–1370. https://doi.org/10.5194/acp-5-1357-2005.
65. Archer J, Kolwas M, Jakubczyk D, Derkachov G, Woźniak M, Kolwas K. 2017. Evolution of radius and light scattering properties of single drying microdroplets of colloidal suspension. J Quant Spectrosc Radiat Transf 202:168–175. https://doi.org/10.1016/j.jqsrt.2017.08.004.
66. Krieger UK, Meier P. 2011. Observations and calculations of two-dimensional angular optical scattering (TAOS) patterns of a single levitated cluster of two and four microspheres. J Quant Spectrosc Radiat Transf 112:1761–1765. https://doi.org/10.1016/j.jqsrt.2011.01.034.
67. Davis EJ. 1997. A history of single aerosol particle levitation. Aerosol Sci Technol 26:212–254. https://doi.org/10.1080/02786829708965426.
68. Thomas RJ, Webber D, Hopkins R, Frost A, Laws T, Jayasekera PN, Atkins T. 2011. The cell membrane as a major site of damage during aerosolization of Escherichia coli. Appl Environ Microbiol 77:920–925. https://doi.org/10.1128/AEM.01116-10.
69. Terzieva S, Donnelly J, Ulevicius V, Grinshpun SA, Willeke K, Stelma GN, Brenner KP. 1996. Comparison of methods for detection and enumeration of airborne microorganisms collected by liquid impingement. Appl Environ Microbiol 62:2264–2272. https://doi.org/10.1128/AEM.62.7.2264-2272.1996.
70. Mainelis G, Adhikari A, Willeke K, Lee SA, Reponen T, Grinshpun SA. 2002. Collection of airborne microorganisms by a new electrostatic precipitator. J Aerosol Sci 33:1417–1432. https://doi.org/10.1016/S0021-8502(02)00091-5.
71. Juozaitis A, Willeke K, Grinshpun SA, Donnelly J. 1994. Impaction onto a glass slide or agar versus impingement into a liquid for the collection and recovery of airborne microorganisms. Appl Environ Microbiol 60:861–870. https://doi.org/10.1128/AEM.60.3.861-870.1994.